High-pressure study of the anomalous ferromagnet $CeRh_3B_2$ to 7 GPa: Comparison with substitutional experiments

A. L. Cornelius and J. S. Schilling
Department of Physics, Washington University, Campus Box 1105, One Brookings Drive, St. Louis, Missouri 63130-4899
(Received 14 June 1993; revised manuscript received 18 October 1993)

The ferromagnet $CeRh_3B_2$ has a Curie temperature T_C near 117 K, two orders of magnitude higher than anticipated from simple de Gennes scaling. To shed light on the nature of the anomalous magnetic state, the hydrostatic pressure dependence of T_C was measured to 7.0 GPa using a diamond-anvil cell with dense He as pressure medium. As a function of pressure, $T_C(P)$ initially increases at the rate of 1.0 K/GPa but then passes through a maximum near 2.5 GPa and falls rapidly at higher pressures. This qualitative behavior can be accounted for by a simple phase diagram proposed some time ago by Doniach for dense Kondo systems. This diagram is also used to compare the evolution of magnetism in related substitutional compounds to that for $CeRh_3B_2$ under pressure. For selected Ce compounds, a universal relation between the coupling strength J and the ordering temperature T_C is found.

I. INTRODUCTION

The ternary boride compound series, RM_3B_2, where R is a rare earth and M belongs to the 4*d* (Rh or Ru) or 5*d* (Os or Ir) transition-metal series, was reported by Ku *et al.*[1] Subsequently, Dhar, Malik, and Vijayaraghavan[2] examined one member of this series, $CeRh_3B_2$, and found it to be ferromagnetic with a Curie temperature of $T_C \simeq 115$ K, the highest magnetic ordering temperature of any Ce compound with nonmagnetic elements and two orders of magnitude higher than the value $T_C \approx 1$ K estimated using simple de Gennes scaling of the Curie temperature (~ 93 K) for the isostructural compound $GdRh_3B_2$. Whereas the saturation moment μ_s of $CeRh_3B_2$ at 77 K and 8 kOe is only $\sim 0.31\mu_B$/Ce,[2] at temperatures well above T_C, the static susceptibility follows Curie-Weiss behavior with $\mu_{\rm eff} \simeq 3.0\mu_B$/Ce and $\theta_p \simeq -373$ K. X-ray diffraction is consistent with the hexagonal $CeCo_3B_2$-type structure (space group $P6/mmm$) with lattice parameters $a = 5.477$ Å and $c = 3.091$ Å. Dhar, Malik, and Vijayaraghavan[2] interpret the anomalously low value of the unit-cell volume compared with the other RRh_3B_2 systems as evidence that Ce in $CeRh_3B_2$ is in a mixed-valent state. However, $L_{\rm III}$-edge x-ray-absorption spectra[3] indicate that the occupancy of the 4*f* level is $n_f \simeq 0.95$, i.e., Ce is nearly trivalent. In view of the fact that the saturation moment μ_s in $CeRh_3B_2$ is small compared to $\mu_{\rm eff}$, Dhar, Malik, and Vijayaraghavan[2] suggest that the magnetism is itinerant in nature and arises from the Rh 4*d* band. However, the small density of Rh 4*d* states at the Fermi energy[3] and the results of substitution experiments[4] clearly show that the ferromagnetism is not itinerant but is due to the ordering of local moments at the Ce sites. Subsequent ^{11}B NMR (Ref. 5) and neutron-diffraction studies[6] confirm this picture. However, the direction of the easy axis of magnetization has not yet been unequivocally established; magnetization[7] and neutron-diffraction[6] studies differ on whether the easy axis is perpendicular or parallel to the *c* axis, respectively.

It has been proposed by several groups that the magnetic behavior of $CeRh_3B_2$ can be explained by considering it to be a dense Kondo system.[3,4,8,9] The magnetic behavior of a dense Kondo system is largely controlled by the strength of the *f*-*d* hybridization V_{df} between the magnetic *f* electrons and the conduction *d* electrons. The exchange-coupling strength J, where $J \propto |V_{df}|^2$, can be varied in $CeRh_3B_2$ by either chemical substitution or the application of pressure. A number of years ago, Doniach[10] examined the one-dimensional (1D) Kondo lattice, or "Kondo necklace," problem in the mean-field approximation and obtained an antiferromagnetic ground state with a simple phase diagram seen in Fig. 1 which gives the magnetic ordering temperature T_C as a function of $|JN(E_F)|$, where $N(E_F)$ is the density of states at the Fermi energy. Application of pressure is known to increase the value of $|JN(E_F)|$ in Ce compounds.[11] With increasing pressure, therefore, T_C would be expected to initially increase, then pass through a maximum and drop precipitously as T_K rapidly overtakes $T_{\rm RKKY}$. In addition, the rapid increase in T_K would be expected to lead to a monotonic decrease in the saturation moment μ_s at a given temperature.[12]

A good deal of theoretical work[13] on one-,[14] two-,[15] and three-dimensional[12] Kondo lattices has been carried out since Doniach's original work. This subsequent work indicates that both antiferromagnetic and ferromagnetic ground states are possible, depending on the extent of band filling, and that the magnetic/nonmagnetic transition, which occurs at $|JN(E_F)| = 1$ in Doniach's mean-field calculation, takes place at significantly lower values of $|JN(E_F)|$. Thus, we should view the Doniach phase diagram in Fig. 1 as only a qualitative description of the functional dependence of T_C on $|JN(E_F)|$. For sufficiently large values of $|JN(E_F)|$, the system enters the mixed-valence regime where the above Kondo lattice models are all of limited validity.

Shaheen *et al.*[16] investigated the pressure dependence

0163-1829/94/49(6)/3955(7)/$06.00

of the magnetization in $CeRh_3B_2$ to 1.2 GPa and found that the Curie temperature *increases* weakly with pressure at the rate $d\ln T_C/dP \simeq +0.9\%/\text{GPa}$, whereas the saturation moment *decreases* at the rapid rate $d\ln\mu_s/dP \simeq -6.6\%/\text{GPa}$. Since $|JN(E_F)|$ increases under pressure, these results would indicate that this compound is situated just to the left of the maximum in the phase diagram in Fig. 1, as shown. It would be useful to extend these measurements to higher pressures to see whether $T_C(P)$ passes through the anticipated maximum. We have determined the Curie temperature of $CeRh_3B_2$ in a diamond-anvil cell as a function of hydrostatic pressures as high as 7.0 GPa. With increasing pressure, the value of T_C initially increases, passes through a maximum near 2.5 GPa, and then decreases rapidly. Above 6.3 GPa, the ferromagnetic transition can no longer be detected in the ac-susceptibility measurements.

II. EXPERIMENT

The polycrystalline $CeRh_3B_2$ sample for the present study was the same as used in previous work[16] and was prepared by argon-arc-melting stoichiometric amounts of high-purity Ames Lab rare earths (≤ 15 ppm of any single metallic impurity) together with commercial rhodium (99.9%, Thiokol Corp., Alfa Products) and boron (99.995%, Research Organic-Inorganic Chemical Corp.). To promote homogeneity, each sample was turned over and remelted six times. Powder x-ray-diffraction studies confirm the anticipated hexagonal ($P6/mmm$) structure with no trace of a secondary phase. The high-pressure techniques used in the present experiments have been described in some detail by Klotz, Schilling, and Müller.[17]

The high-pressure apparatus consists of a copper-beryllium diamond-anvil clamp using $\frac{1}{6}$ carat diamonds with 0.5-mm culets. Gaskets of TaW with diameter 3 mm and thickness ~ 300 μm are preindented to ~ 120 μm. The sample with volume $\sim 10^{-4}$ mm^3 is placed together with small pieces of ruby in a 250-μm-diam hole drilled through the center of the gasket. The pressure clamp is placed in a continuous flow cryostat; superfluid ^{4}He is loaded into the gasket hole at 2 K to serve as pressure medium. The pressure in the gasket hole is changed at a temperature above the melting curve of He by loading a membrane[18] with helium gas to force the diamonds together. The magnitude of the pressure in the cell is determined by the standard ruby fluorescence technique.[19] The Curie temperature is detected inductively by a sensitive measurement of the ac susceptibility $\chi_{ac}(T)$, using a PAR 124 lock-in amplifier, as a function of slowly varying temperature (0.3–0.5 K/min). After the subtraction of a temperature-dependent background from $\chi_{ac}(T)$, the ferromagnetic transition becomes clearly visible; the onset of the transition is used to define T_C.[17]

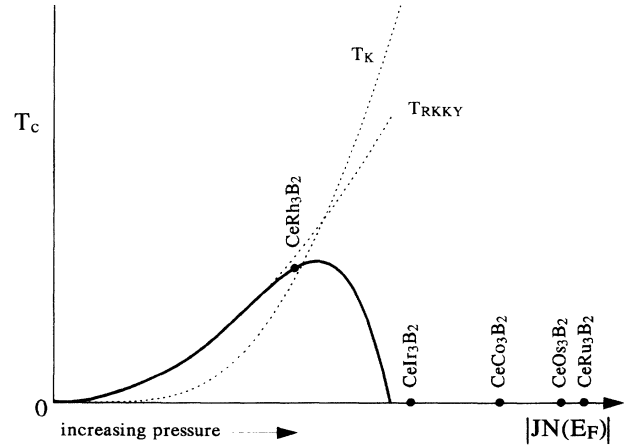

FIG. 1. The phase diagram of the one-dimensional "Kondo necklace" adapted from Ref. 10. T_{RKKY} is the temperature associated with the RKKY interaction energy, T_K the Kondo temperature, T_C the magnetic ordering temperature, J the coupling strength and $N(E_F)$ the density of states at the Fermi energy. The approximate positions of the compounds CeM_3B_2 (M = Rh, Ir, Co, Os, and Ru) are indicated (●), as discussed in the text. The position of a given Ce system in this diagram moves to the right as pressure is applied.

III. RESULTS

The pressure dependence of T_C for $CeRh_3B_2$ was determined in four different experiments on four distinct pieces from the same sample. The four pieces studied all exhibit a zero-pressure value of the Curie temperature given by $T_C \simeq 118.2 \pm 0.2$ K. In Fig. 2, T_C is seen to initially increase as pressure is applied, but then to decrease at higher pressures. In Fig. 3 we give an overview of the dependence of T_C on pressure for all four pieces studied. After an initial increase in T_C under pressure to 2.5 GPa at the rate $dT_C/dP \simeq +1.0 \pm 0.3$ K/GPa, a value comparable to that obtained by Shaheen *et al.*,[16] $T_C(P)$ is seen to pass through a maximum and then decrease rapidly; no transition could be detected above 6.3 GPa. The $T_C(P)$ curve was found to be reversible in pressure, with the value of T_C for all samples returning to the same value at zero pressure. Since $|JN(E_F)|$ increases under pressure for Ce compounds, these results are fully consistent with the conclusions of the earlier experiments[16]

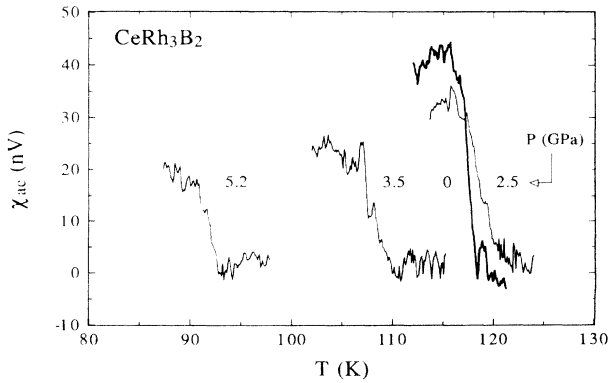

FIG. 2. Measured ac-susceptibility signal in nanovolts versus temperature at various pressures for a ~ 1-μg sample of $CeRh_3B_2$. The applied ac field is 20 Oe at 820 Hz. With increasing pressure, the onset temperature of the ferromagnetic transition is seen to first rise but then fall.

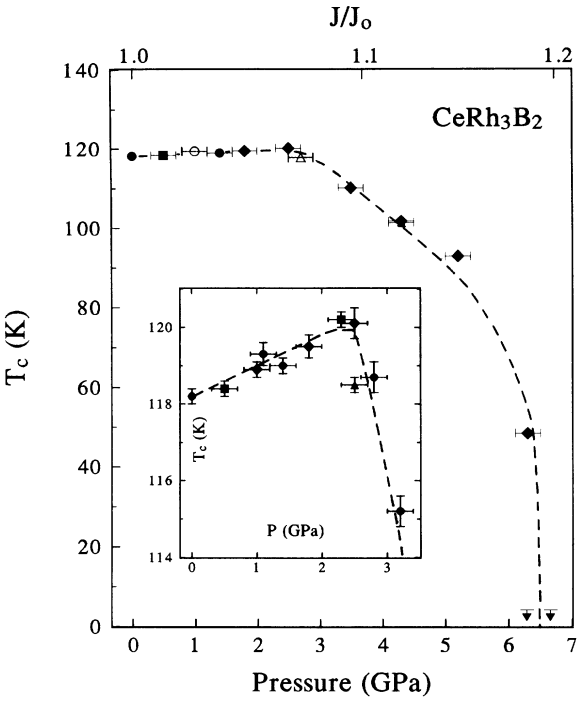

FIG. 3. The dependence of the Curie temperature T_C of $CeRh_3B_2$ on hydrostatic pressure to 7 GPa. For clarity only a fraction of all data is shown. The closed (open) symbols represent measurements made for increasing (decreasing) pressure during four separate runs on four different pieces from the same sample. The error bars for T_C are smaller than the symbols. The upper horizontal scale gives the relative coupling strength J/J_0 (see text). The inset shows on an expanded scale all measurement made with increasing pressure to 3.5 GPa. The dashed lines are guides to the eye.

that $CeRh_3B_2$ is a dense Kondo system positioned just to the left of the maximum in the phase diagram in Fig. 1. The present pressure range is sufficient not only to push the magnetic ordering temperature through a maximum, but also to drive the sample past the magnetic-nonmagnetic transition near 6.3 GPa.

The effect of volume change on the magnetism of $CeRh_3B_2$ has also been studied by Malik *et al.*[8] in chemical pressure experiments in the $CeRh_3(B_{1-y}Si_y)_2$ series by substituting Si for B to expand the lattice. Expanding the lattice would be expected to decrease the magnitude of the coupling strength J and cause the system to move to the left in Fig. 1. The results given in Fig. 4(a) for the dependence of both T_C and the saturation moment μ_s on y confirm this expectation. With increasing y, T_C decreases, whereas the saturation moment increases. The deviation in $\mu_s(y)$ from the extrapolated line for $y > 0.3$ may arise from the fact that the temperature at which μ_s is determined (~ 4 K) is not sufficiently low compared to the Curie temperature $T_C \simeq 15$ K.

We now compare these results with those from chemical substitution experiments on the Rh site. The magnetic state in $CeRh_3B_2$ can be altered by replacing Rh by other transition metals in $Ce(Rh_{1-x}M_x)_3B_2$ (M=Ru, Ir, Co, or Os).[4,8,9,20–23] The ground states of these compounds are quite diverse: $CeRh_3B_2$ is ferromagnetic, $CeIr_3B_2$, the only member that does not crystallize in the hexagonal structure[22] is mixed valent, $CeCo_3B_2$ is nonmagnetic, and $CeRu_3B_2$ and CeO_3B_2 are superconducting. Whereas $CeRh_3B_2$ is positioned to the left of the maximum in Fig. 1, the other four compounds are positioned to the right of the magnetic-nonmagnetic boundary since they are all nonmagnetic. Since for $Ce(Rh_{1-x}Ru_x)_3B_2$, the magnetic-nonmagnetic transition occurs at $x \sim 0.1$ the smallest value of x for any of the CeM_3B_2 compounds, $CeRu_3B_2$ should lie farthest to the right. The other compounds are placed to the left of $CeRu_3B_2$ in increasing order of the degree of substitution x required to reach the magnetic-nonmagnetic boundary. Substitution of a concentration x of any of the transition metals M=Ru, Ir, Co, or Os for Rh would be expected to cause an increase in $|JN(E_F)|$ and thus mimic the effect of high pressure, i.e., with increasing x, $\mu_s(x)$ decreases, whereas $T_C(x)$ passes through a maximum. This behavior, in fact, has been observed for $Ce(Rh_{1-x}Ir_x)_3B_2$ by Hsu and Ku,[9] as seen in Fig. 4(b), where $T_C(P)$ is seen to pass through a maximum at $x=0.3$. For the corresponding series with M=Co, Ru, or Os, the data in Figs. 4(c) and 4(d) are not spaced closely enough to show unequivocally that $T_C(x)$ passes through the maximum indicated by the lines drawn in the figures. However, the saturation moment $\mu_s(x)$ does decrease with increasing x, but at a rate 3× and 10× more rapidly for Co (Ref. 23) and Ru or Os substitution (Refs. 4, 20, and 21) compared to Ir substitution, respectively.

Utilizing chemical substitution, therefore, it is possible to cause $|JN(E_F)|$ for $CeRh_3B_2$ to either *increase* by substituting a transition metal (M=Ir, Co, Ru, or Os) for Rh or *decrease* by expanding the lattice through Si substitution for B. The above chemical substitution experiments on $CeRh_3B_2$ seem to yield the qualitative behavior of $T_C(x)$ and $\mu_s(x)$ anticipated for a dense Kondo system which lies for $x=0$ just to the left of the maximum in the phase diagram in Fig. 1. We now attempt a more quantitative comparison of the chemical substitution and high-pressure experiments.

IV. DISCUSSION

Dense Kondo (or Kondo lattice) systems are characterized by a competition between the magnetic ordering of local moments through Ruderman-Kittel-Kasuya-Yosida (RKKY) interactions and the eventual destruction of the local moments by the Kondo effect. The energies of these competing phenomena are characterized by $T_K \propto N(E_F)^{-1}\exp(1/|JN(E_F)|)$, the binding energy of the Kondo singlet, and $T_{RKKY} \propto J^2N(E_F)$, the energy of the RKKY interaction. For small values of $|JN(E_F)|$, the RKKY term dominates and magnetic ordering will occur. For large values of $|JN(E_F)|$, the Kondo term dominates and the magnetic ordering is destroyed due to Kondo compensation. In Doniach's solution[10] for the one-dimensional "Kondo necklace" in the limit of very

weak coupling, i.e., $|JN(E_F)| \ll 1$, the ordering temperature increases initially as $T_C \propto J^2N(E_F)$. With increasing $|JN(E_F)|$, T_C eventually passes through a maximum and then falls rapidly, approaching zero as $T_C \propto (1-|JN(E_F)|)$. In contrast, the saturation moment μ_s decreases monotically with increasing $|JN(E_F)|$ over the entire range.[12]

As hypothesized by Doniach,[10] this general behavior for a 1D system may even hold for 3D systems. In fact, the phase diagram in Fig. 1 has been used to account for the experimental results on a variety of Ce-based systems that display a well-defined maximum in T_C, including, for example, high-pressure studies on CeAg,[24] and high-pressure and substitution experiments on CeM_2X_2

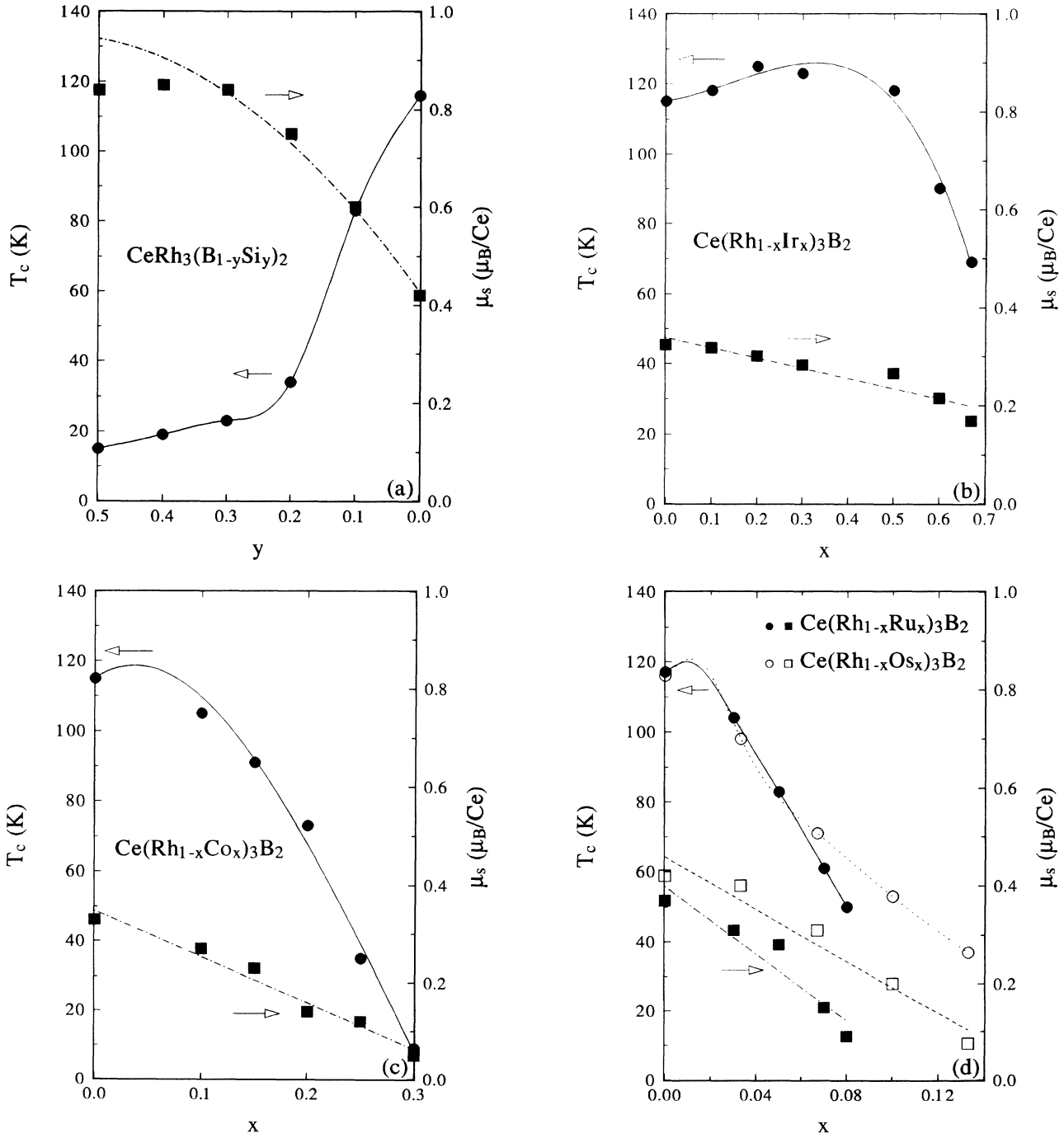

FIG. 4. The Curie temperature T_C (●) and the saturation moment μ_s (■) as a function of x or y for (a) $CeRh_3(B_{1-y}Si_y)_2$ from Ref. 8 (μ_s at 4 K and 5 kOe), (b) $Ce(Rh_{1-x}Ir_x)_3B_2$ from Ref. 9 (μ_s at 5 K and 10 kOe), (c) $Ce(Rh_{1-x}Co_x)_3B_2$ from Ref. 23 (μ_s at 5 K and 10 kOe), and (d) $Ce(Rh_{1-x}Ru_x)_3B_2$ (closed symbols) from Ref. 4 (μ_s at 5 K and 8 kOe) and $Ce(Rh_{1-x}Os_x)_3B_2$ (open symbols) from Ref. 21 (μ_s at 5 K and 50 kOe). All lines are guides to the eye. The maxima in the $T_C(x)$ curves in (c) and (d) are drawn to facilitate the discussion in the text; the data density is insufficient to reveal the maxima.

(M=Ag, Au, Pd, or Rh; X=Si or Ge),[25–27] $CeSi_x$,[16] and $CePt_{1-x}Ni_x$.[28,29] More recently, Endstra, Nieuwenhuys, and Mydosh[30] have combined the Doniach phase diagram with the ideas of Harrison and Straub[31–33] to categorize the magnetic behavior of a sizable number of Ce and U compounds. They use the Schrieffer-Wolf expression[34]

$$J_{df}=\frac{-2|V_{df}|^2}{E_F-E_f} \tag{1}$$

to relate the coupling strength J_{df} to the hybridization between the localized f electrons and the conduction d electrons, where V_{df} is the d-f hybridization and E_f is the energy of the f level. According to Harrison and Straub,[31–33] for an isostructural series V_{df} is given by $V_{df}\propto\sqrt{(r_f^5 r_d^3)/d^6}$, where r_f and r_d are the atomic radii of the f and d atoms, respectively, and d is the separation between them. These radii are derived from the muffin-tin orbital bandwidths of pure f and d metals.[32] Endstra, Nieuwenhuys, and Mydosh[30] calculated relative values of V_{df} for a given Ce or U series, and using Doniach's phase diagram, were able to successfully categorize the various members of a given system according to their values of V_{df}. If the $4f$ level is pinned at the Fermi energy, i.e., E_F-E_f is constant, Eq. (1) tells us that the value of J_{df} should depend only on the atomic radii and the separation of the f and d atoms in the manner given by

$$J_{df}\propto|V_{df}|^2\propto\frac{r_f^5 r_d^3}{d^{12}}\ . \tag{2}$$

We now use Eq. (2) to estimate the change in J_{df} under pressure for $CeRh_3B_2$. The separation between Ce and Rh in this hexagonal compound is given by $d=(\sqrt{a^2+c^2})/2$, where a and c are the lattice parameters. In both the high-pressure and the substitution experiments, the values of r_f and r_d are assumed to remain unchanged. If the $4f$ level is pinned at the Fermi energy, as was observed by Allen *et al.*[35] for the $Ce(Rh_{1-x}Ru_x)_3B_2$ series, then the value of J relative to that for $CeRh_3B_2$ will be given by

$$\frac{J}{J_0}=\left[\frac{a_0^2+c_0^2}{a^2+c^2}\right]^6\left[\frac{r_d^3}{r_{\mathrm{Rh}}^3}\right], \tag{3}$$

where a_0 and c_0 are the ambient pressure values of the lattice parameters for $CeRh_3B_2$, and r_d^3 and r_{Rh}^3 are the averaged cubed values of the d-atom radius at the transition-metal site and the cube of the atomic radius of Rh, respectively.[32] If we assume the compressibility is isotropic, the pressure-dependent values for a and c are given by

$$a=a_0\left[1+\frac{\Delta V}{3V}\right]\ \text{and}\ c=c_0\left[1+\frac{\Delta V}{3V}\right], \tag{4}$$

where $\Delta V=V-V_0$ is the change in volume. The initial values of the lattice parameters are $a_0=5.472$ Å and $c_0=3.094$ Å.[4] Setting $B'\simeq 4$,[36] the Birch equation of state is given by

$$V=V_0\left[\frac{4P}{B}+1\right]^{-1/4}, \tag{5}$$

where P is the pressure and the bulk modulus is equal to $B=141$ GPa.[37]

The dependence of both T_C/T_{C0} and μ_s on J/J_0 can now be calculated using Eq. (3) for both the high-pressure and the substitution experiments;[4,8,9] the results are displayed in Fig. 5. The results for both the present pressure measurements on $CeRh_3B_2$ and the Ir- and Si-substitution experiments are seen to be in reasonably good agreement with each other, as well as with the qualitative dependence given in the phase diagram in Fig. 1, where for constant $N(E_F)$, T_C initially increases with increasing $|J|$ with an apparent positive curvature, followed by a maximum and a subsequent rapid drop when approaching the magnetic-nonmagnetic phase transition.

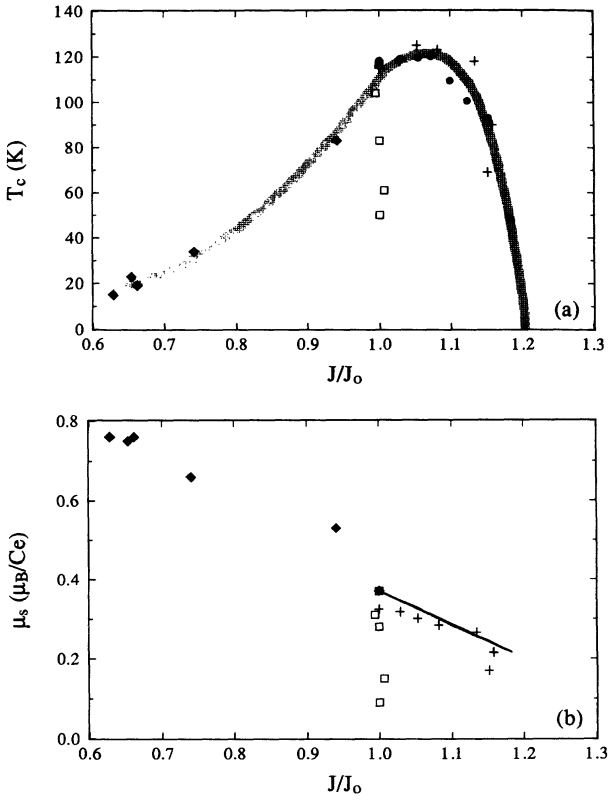

FIG. 5. (a) The dependence of the Curie temperature T_C on the coupling strength J, normalized to its value J_0 for $CeRh_3B_2$ at ambient pressure, for the current high-pressure experiment on $CeRh_3B_2$ (●), and substitution experiments on $CeRh_3(B_{1-y}Si_y)_2$ (◇), $Ce(Rh_{1-x}Ir_x)_3B_2$ (+), and $Ce(Rh_{1-x}Ru_x)_3B_2$ (□). With the exception of $Ce(Rh_{1-x}Ru_x)_3B_2$, the data roughly follow a curve represented by the shaded region which resembles the qualitative phase diagram in Fig. 1, where $T_C\propto J^2$ for small J. (b) The dependence of the saturation moment μ_s on the coupling strength J normalized to its value J_0 for $CeRh_3B_2$ at ambient pressure. The high-pressure data from Ref. 12 are represented by a solid line corresponding to the dependence $d\ln\mu_s/dP=-6.6\%/\mathrm{GPa}$. Except for $Ce(Rh_{1-x}Ru_x)_3B_2$, the data roughly follow a linear dependence given by the shaded region.

This would imply that the variation of the magnetic state in these experiments can be understood primarily as arising from changes in J alone; apparently, the changes in $N(E_F)$ are negligible compared to those of J. In contrast, in Fig. 5 it is seen that the data for Ru substitution are in poor agreement. The same poor agreement is also obtained for $Ce(Rh_{1-x}Os_x)_3B_2$ and $Ce(Rh_{1-x}Co_x)_3B_2$ which are not shown in Fig. 5. For these latter two systems, it appears that $N(E_F)$ may vary significantly with x and/or our assumption that $E_F - E_f$ is constant is incorrect. It is interesting to note that Allen *et al.*[35] have shown that $N(E_F)$ increases by more than a factor of 2 from $CeRh_3B_2$ to $CeRu_3B_2$.

In relatively few Ce systems has the magnetic ordering temperature been found to pass through a maximum as a function of the lattice parameter without substituting for the d-metal atom. In addition to this work on $CeRh_3B_2$, these systems include the substitution of Ge for Si in CeM_2Si_2 (M=Pd, Rh, or Ru) (Refs. 25, 26, and 38), as well as high-pressure work on CeAg.[24] The compounds CeM_2X_2 (M=Pd, Rh, Ru, or Cu; X=Ge or Si) crystallize in the tetragonal $ThCr_2Si_2$-type structure and display interesting magnetic behavior. $CePd_2Si_2$ orders antiferromagnetically at $T_C=10$ K, a value comparable to that of the isostructural Gd compound with $T_C \approx 13$ K.[39] $CeRh_2Si_2$ orders antiferromagnetically at $T_C=37$ K, the second highest ordering temperature of any Ce compound with nonmagnetic elements ($CeRh_3B_2$ has the highest). $CeRu_2Ge_2$ is ferromagnetic at $T_C=9$ K, but Si substitution changes the ordering to antiferromagnetic with the end member $CeRu_2Si_2$ being nonmagnetic.[38] $CeCu_2Si_2$ is a heavy-fermion superconductor below 0.6 K; its structure has been studied to pressures of 30 GPa, and the bulk modulus was determined to be 110 GPa.[40] The magnetic ordering temperatures of all systems $CeM_2(Si_{1-x}Ge_x)_2$ with M=Pd, Rh, or Ru are observed to pass through a maximum at some value of x.[25,26,38] The magnetic ordering temperature for M=Pd or Rh has been found by Thompson, Parks, and Borges[27] to decrease rapidly with applied pressure to 1.4 GPa. The CsCl-structure compound CeAg exhibits ferromagnetic order below $T_C=5.6$ K; $T_C(P)$ passes through a maximum at 0.7 GPa.[24]

We have calculated from Eq. (3) the relative change in J for the above compounds using the published lattice parameters for the substitution experiments and assuming isotropic compression for the pressure experiments. We use the Birch equation of state with $B=110$ GPa for CeM_2Si_2 (Ref. 40) and $B=57$ GPa for CeAg (Ref. 41). In Fig. 6 the normalized ordering temperature $T_C/T_{C,\max}$ is plotted versus $J/J_{T_{C,\max}}$, where $J_{T_{C,\max}}$ is the value of the coupling constant which gives the maximum ordering temperature $T_{C,\max}$. The observed dependence is seen to generally be in approximate agreement with that for $CeRh_3B_2$. As can be seen, all systems can be mapped reasonably well onto a Doniach-like universal curve. This apparent universality is particularly significant in view of the fact that for the compounds shown there is appreciable variation in the ordering temperatures, the type of magnetic order, and the crystal structures.

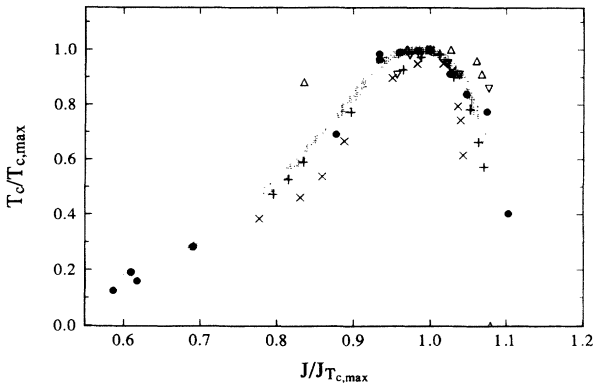

FIG. 6. The magnetic ordering temperature versus the coupling strength for five different Ce compounds. Both quantities have been normalized to their values where T_C is a maximum. The systems displayed are (●) $CeRh_3B_2$ (F, $T_C=117$ K), (×) $CeRh_2Si_2$ (AF, $T_C=37$ K), (+) $CePd_2Si_2$ (AF, $T_C=10$ K), (△) $CeRu_2Si$ (nonmagnetic), and (▽) CeAg (F, $T_C=5.6$ K), where F represents ferromagnetic and AF represents antiferromagnetic ordering. The shaded region is identical to the one used in Fig. 5(a) and resembles the qualitative phase diagram in Fig. 1.

ACKNOWLEDGMENTS

The authors would like to thank J. A. Mydosh for stimulating discussions and for providing a copy of the work in Ref. 30 on which much of the present analysis is based. We are also grateful to T. Endstra for sending us a copy of his Ph.D. dissertation.

[1]H. C. Ku, G. P. Meisner, F. Acker, and D. C. Johnston, Solid State Commun. **35**, 91 (1980).
[2]S. K. Dhar, S. K. Malik, and R. Vijayaraghavan, J. Phys. C **14**, L321 (1981).
[3]E. V. Sampathkumaran, G. Kaindl, C. Laubschat, W. Krone, and G. Worthmann, Phys. Rev. B **31**, 3185 (1985).
[4]S. A. Shaheen, J. S. Schilling, and R. N. Shelton, Phys. Rev. B **31**, 656 (1985).
[5]Y. Kitaoka, Y. Kishimoto, K. Asayama, T. Kohara, K. Takeda, R. Vijayaraghavan, S. K. Malik, S. K. Dhar, and D. Ranbabu, J. Magn. Magn. Mater. **52**, 449 (1985).
[6]A. C. Lawson, A. Williams, and J. G. Huber, J. Less-Common Met. **136**, 87 (1987).
[7]M. Kasaya, A. Okabe, T. Takahashi, T. Satoh, T. Kasuya, and A. Fujimori, J. Magn. Magn. Mater. **76&77**, 347 (1988).
[8]S. K. Malik, G. K. Shenoy, S. K. Dhar, P. L. Paulose, and R. Vijayaraghavan, Phys. Rev. B **34**, 8196 (1986).
[9]S. W. Hsu and H. C. Ku, Phys. Rev. B **38**, 2944 (1988).

[10]S. Doniach, in *Valence Instability and Related Narrow Band Phenomena,* edited by R. D. Parks (Plenum, New York, 1977).
[11]J. S. Schilling, Adv. Phys. **28**, 657 (1979).
[12]C. Lacroix and M. Cyrot, Phys. Rev. B **20**, 1969 (1979).
[13]See, C. Lacroix, J. Magn. Magn. Mater. **100**, 90 (1991), and references within.
[14]P. Santini and J. Sólyom, Phys. Rev. B **46**, 7422 (1992).
[15]P. Fazekas and E. Müller-Hartmann, Z. Phys. B **85**, 285 (1991).
[16]S. A. Shaheen, J. S. Schilling, P. Klavins, C. B. Vining, and R. N. Shelton, J. Magn. Magn. Mater. **47&48**, 285 (1985); S. A. Shaheen, J. S. Schilling, M. Abd-Elmeguid, H. Micklitz, P. Klavins, and R. N. Shelton, Physica B **139&140**, 410 (1986).
[17]S. Klotz, J. S. Schilling, and P. Müller, in *Frontiers on High-Pressure Research,* edited by H. D. Hochheimer and E. D. Etters (Plenum, New York, 1991).
[18]W. B. Daniels and W. Ryschkewitsch, Rev. Sci. Instrum. **54**, 115 (1983).
[19]G. J. Piermarini, S. Block, J. D. Barnett, and R. A. Forman, J. Appl. Phys. **46**, 2774 (1975).
[20]M. B. Maple, S. E. Lambert, M. S. Torikachvili, K. N. Yang, J. W. Allen, B. B. Pate, and I. Lindau, J. Less-Common Met. **111**, 239 (1985).
[21]S. K. Malik, A. M. Umarji, G. K. Shenoy, and M. E. Reeves, Solid State Commun. **54**, 761 (1985).
[22]A. M. Umarji, S. K. Dhar, S. K. Malik, and R. Vijayaraghavan, Phys. Rev. B **36**, 8929 (1987).
[23]H. Yu and H. C. Ku, Jpn. J. Appl. Phys. **26-3**, 561 (1987).
[24]A. Eiling and J. S. Schilling, Phys. Rev. Lett. **46**, 364 (1981).
[25]C. Godart, L. C. Gupta, C. V. Tomy, J. D. Thompson, and R. Vijayaraghavan, Europhys. Lett. **8**, 375 (1989).
[26]I. Das and E. V. Sampathkumaran, Phys. Rev. B **44**, 9711 (1991).
[27]J. D. Thompson, R. D. Parks, and H. Borges, J. Magn. Magn. Mater. **54-57**, 377 (1986).
[28]D. Gignoux and J. Voiron, J. Magn. Magn. Mater. **54-57**, 363 (1986).
[29]D. Gignoux and J. C. Gomez-Sal, Phys. Rev. B **30**, 3967 (1984).
[30]T. Endstra, G. J. Nieuwenhuys, and J. A. Mydosh, Phys. Rev. B **48**, 9595 (1993); T. Endstra, Ph.D. thesis, University of Leiden, 1992.
[31]W. A. Harrison, Phys. Rev. B **28**, 550 (1983).
[32]G. K. Straub and W. A. Harrison, Phys. Rev. B **31**, 7668 (1985).
[33]W. A. Harrison and G. K. Straub, Phys. Rev. B **36**, 2695 (1987).
[34]J. R. Schrieffer and P. A. Wolff, Phys. Rev. **149**, 491 (1966).
[35]J. W. Allen, M. B. Maple, J.-S. Kang, K. N. Yang, M. S. Torikachvili, Y. Lassailly, W. P. Ellis, B. B. Pate, and I. Lindau, Phys. Rev. B **41**, 9013 (1990).
[36]A. M. Hofmeister, J. Geophys. Res. **96**, 21 893 (1991).
[37]K. S. Athreya, Ph.D. thesis, Iowa State University, 1986.
[38]S. Dakin, G. Rapson, and B. D. Rainford, J. Magn. Magn. Mater. **108**, 117 (1992).
[39]I. Das and E. V. Sampathkumaran, Solid State Commun. **81**, 905 (1992).
[40]I. L. Spain, F. Steglich, U. Rauchschwalbe, and H. D. Hochheimer, Physica B **139-140**, 449 (1986).
[41]M. Kurisu, J. Phys. Soc. Jpn. **56**, 4064 (1987).

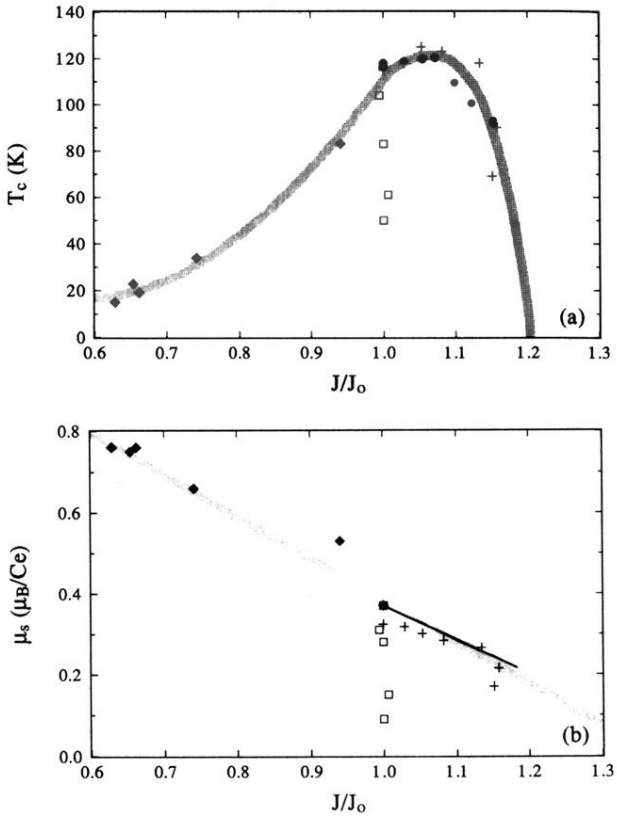

FIG. 5. (a) The dependence of the Curie temperature T_C on the coupling strength J, normalized to its value J_0 for $CeRh_3B_2$ at ambient pressure, for the current high-pressure experiment on $CeRh_3B_2$ (●), and substitution experiments on $CeRh_3(B_{1-y}Si_y)_2$ (◇), $Ce(Rh_{1-x}Ir_x)_3B_2$ (+), and $Ce(Rh_{1-x}Ru_x)_3B_2$ (□). With the exception of $Ce(Rh_{1-x}Ru_x)_3B_2$, the data roughly follow a curve represented by the shaded region which resembles the qualitative phase diagram in Fig. 1, where $T_C \propto J^2$ for small J. (b) The dependence of the saturation moment μ_s on the coupling strength J normalized to its value J_0 for $CeRh_3B_2$ at ambient pressure. The high-pressure data from Ref. 12 are represented by a solid line corresponding to the dependence $d\ln\mu_s/dP = -6.6\%/\text{GPa}$. Except for $Ce(Rh_{1-x}Ru_x)_3B_2$, the data roughly follow a linear dependence given by the shaded region.

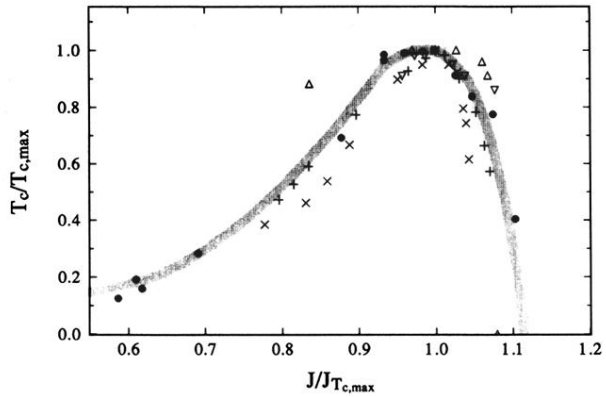

FIG. 6. The magnetic ordering temperature versus the coupling strength for five different Ce compounds. Both quantities have been normalized to their values where T_C is a maximum. The systems displayed are (●) $CeRh_3B_2$ (F, $T_C=117$ K), (×) $CeRh_2Si_2$ (AF, $T_C=37$ K), (+) $CePd_2Si_2$ (AF, $T_C=10$ K), (△) $CeRu_2Si$ (nonmagnetic), and (▽) CeAg (F, $T_C=5.6$ K), where F represents ferromagnetic and AF represents antiferromagnetic ordering. The shaded region is identical to the one used in Fig. 5(a) and resembles the qualitative phase diagram in Fig. 1.